CALCULATED ENERGY DEPOSITS FROM THE DECAY OF TRITIUM AND OTHER RADIOISOTOPES INCORPORATED INTO BACTERIA

RICHARD BOCKRATH, STANLEY PERSON, *and* FRED FUNK

From the Biophysics Department, The Pennsylvania State University, University Park, Pennsylvania 16802. Dr. Bockrath's present address is the Department of Microbiology, Indiana University Medical Center, Indianapolis, Indiana 46202. Dr. Funk's present address is Biology Division, California Institute of Technology, Pasadena, California 91109.

ABSTRACT Transmutation of the radioisotope tritium occurs with the production of a low energy electron, having a range in biological material similar to the dimensions of a bacterium. A computer program was written to determine the radiation dose distributions which may be expected within a bacterium as a result of tritium decay, when the isotope has been incorporated into specific regions of the bacterium. A nonspherical model bacterium was used, represented by a cylinder with hemispherical ends. The energy distributions resulting from a wide variety of simulated labeled regions were determined; the results suggested that the nuclear region of a bacterium receives on the average significantly different per decay doses, if the labeled regions were those conceivably produced by the incorporation of thymidine-^{3}H, uracil-^{3}H, or ^{3}H-amino acids. Energy distributions in the model bacterium were also calculated for the decay of incorporated ^{14}carbon, ^{35}sulfur, and ^{32}phosphorous.

INTRODUCTION

Tritium as well as other radioisotopes incorporated into bacteria produce definite biological effects upon decay. Explanations for these results are sometimes based on a local effect produced by molecular rearrangements at the site of the transmuted nuclide or the energetic recoil of the nuclide (1). In other instances the beta particles emitted by the transmutation, acting to ionize or otherwise alter cellular material, are considered to cause the observed results by a radiation effect (2). Because the energies of beta particles from tritium (^{3}H) are small, 18 kev and less, the densities of ionizations along the paths of emitted electrons are so great that within the dimensions of a bacterium many primary ionizations occur for every transmutation event. Hence, the radiation component of tritium decay is particularly suspect wherever tritium has been demonstrated to produce biological effects.

Indeed, analytical calculations using a spherical approximation as the model bac-

terium predict radiation doses as a consequence of tritium decay roughly sufficient to account for the known killing efficiencies of tritium in terms of radiation damage (3–5). Moreover, differential dose rates per decay to the bacterial nucleus as a consequence of differential geometries of different incorporated compounds have been suggested (5) to explain the differential killing efficiencies associated with the decay of incorporated thymidine-^{3}H, uracil-^{3}H, and ^{3}H-amino acids (6, 7).

There is at least one example of a local effect produced by tritium decay (8). Thus there is reason to be careful when assigning explanation to phenomenon produced by this isotope. So as to know more precisely what sorts of energy distributions might be expected from different tritium compounds incorporated into specific regions of the bacterium, we have calculated energy distributions from tritium decay using a nonspherical bacterial model, of size and shape approximating that of *E. coli* used in experimental studies. We have recorded energy distributions appropriate for a variety of incorporation configurations. In addition, we have calculated energy distributions for other radioisotopes, ^{14}carbon, ^{35}sulfur, and ^{32}phosphorous.

METHOD

The Rationale

A point source of tritium beta particles would cause energy to be deposited in the material surrounding the source. The distribution of transferred energy would be spherically symmetrical about the point source because the emitted beta particles start in random directions. Therefore, a solid angle having the point source at its apex would enclose a *representative energy sample*. This representative energy sample would be identical to samples enclosed by any orientation of the solid angle about the point source, and the energy distribution along the length of the representative energy sample would be identical to that in any other orientation of the solid angle. The energy distribution would be a function of radial distance, only.

The summation of many representative energy samples randomly oriented about a collection of points would approximate the distribution of energy produced about a collection of tritium point sources. If the points of the collection were selected from some specific region of a volume representing a bacterial cell, and if the energies along each representative energy sample, of many such samples oriented about the points of the collection, were recorded in regions of space representing well defined portions of the model bacterium, a good approximation of the energy distribution produced by tritium in *E. coli* could be derived. The approximation would be improved by including very many representative energy samples.

The Computer Program

A computer program was written to utilize this rationale. The bacterium was simulated by a cylinder with hemispherical ends. The cylinder length was represented by L and the radius (for both the cylinder and hemispheres) by R (Fig. 1*a*). *Labeled regions* within the bacterial volume were defined by the same parameters of cylinder length and radius. The length was always equal to L, while the radial distance had two values r_1 and r_2, with the condition that $0 \leqq r_1 \leqq r_2 \leqq R$. A collection of point sources could be randomly selected within a given labeled region.

The bacterial volume was divided into eight equal *sensing volumes* by seven surfaces within

the bacterial volume, each surface being defined by a specific radial value and the value L for cylinder length (Fig. 1*b*).

In operation the program caused the production of a straight line originating from one of the points of a collection selected randomly in a given labeled region. The line was oriented in a random direction. The line was generated by consecutive steps of 0.1 μ. After each step the position of the end point was located either in one of the specific sensing volumes or external to the bacterial volume, and a quantity of energy was tallied for the sensing volume in which the point was located. The amount of energy recorded after each step was taken from the energy distribution along the representative energy sample. After completing one line to the extent that negligible energy was being tallied (well outside the bacterial volume), a second line was constructed from a second point and the procedure was recycled.

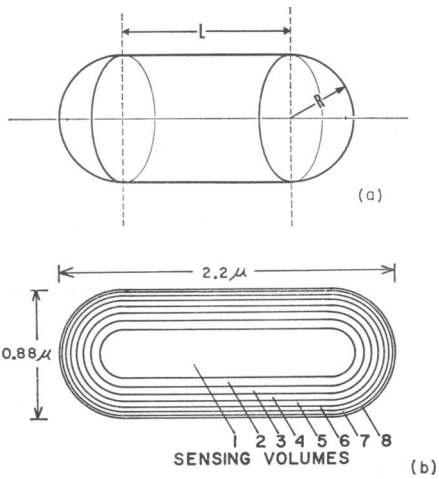

FIGURE 1 The model bacterium. (*a*) A cylinder with hemispherical ends was used as an approximation of the bacterium *Escherichia coli*. The cylinder length (L) was 1.32 μ and the radius (R), common to both cylinder and hemispheres, was 0.44 μ. The total volume was 1.16 μ^3. (*b*) The bacterial volume was divided into eight sensing volumes of equal volume (0.145 μ^3), numbered consecutively from the axis to periphery. These volumes were formed within the bacterial volume by seven surfaces defined by radial values of 0.172, 0.238, 0.285, 0.325, 0.358, 0.388, and 0.414 μ.

1500 cycles of this procedure gave a total distribution of energy, as recorded in the eight sensing volumes and the space external to the bacterial volume, which showed no significant relative variation if supplemented by additional cycles. Thus, one total distribution of transferred energy was approximated by 1500 representative energy samples oriented randomly from points selected randomly within a given labeled region.

Representative Energy Distribution

Of primary importance to the method of the program was a correct representation for the distribution of transferred energy along one representative energy sample. This was to be analogous to a solid angle sampling of the energy transferred to material around a point source of tritium beta particles.

For tritium there seemed to be no experimental data available on the total transferred energy around a point source. Consequently, an expression was calculated after a method previously published (9). According to this method experimental data on the energy transfer of monoenergetic electrons, recorded for electrons having a variety of initial energies, may be added together to construct a generalized energy distribution, called here the *representative energy distribution*. The contribution of each monoenergetic distribution is weighted accord-

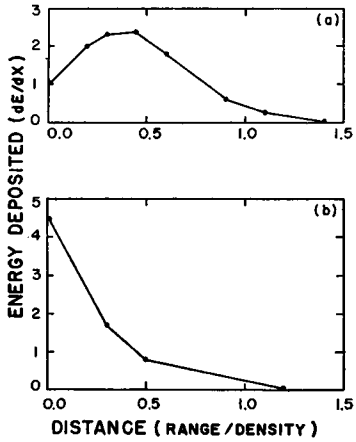

FIGURE 2 Approximate expressions for energy deposition by low energy electrons in absorbing material. Two expressions were used to represent energy absorbed from electrons as a function of depth in absorbing material. The expressions were derived from unpublished data by Dr. A. Cole. (*a*) The expression for electrons of initial energies less than 5 kev. (*b*) The expression for electrons of initial energies equal to or greater than 5 kev. Units of the ordinate were determined by the equation: dE/dx (kev per 100 $\mu g/cm^2$) = $14.5(E + 0.400)^{-0.761}$; and units of the abscissa by: Range (100 $\mu g/cm^2$) = $0.0385(E + 0.400)^{1.77} - 0.0075$ and a density of 1.08 g/cc. E (kev) was the initial energy.

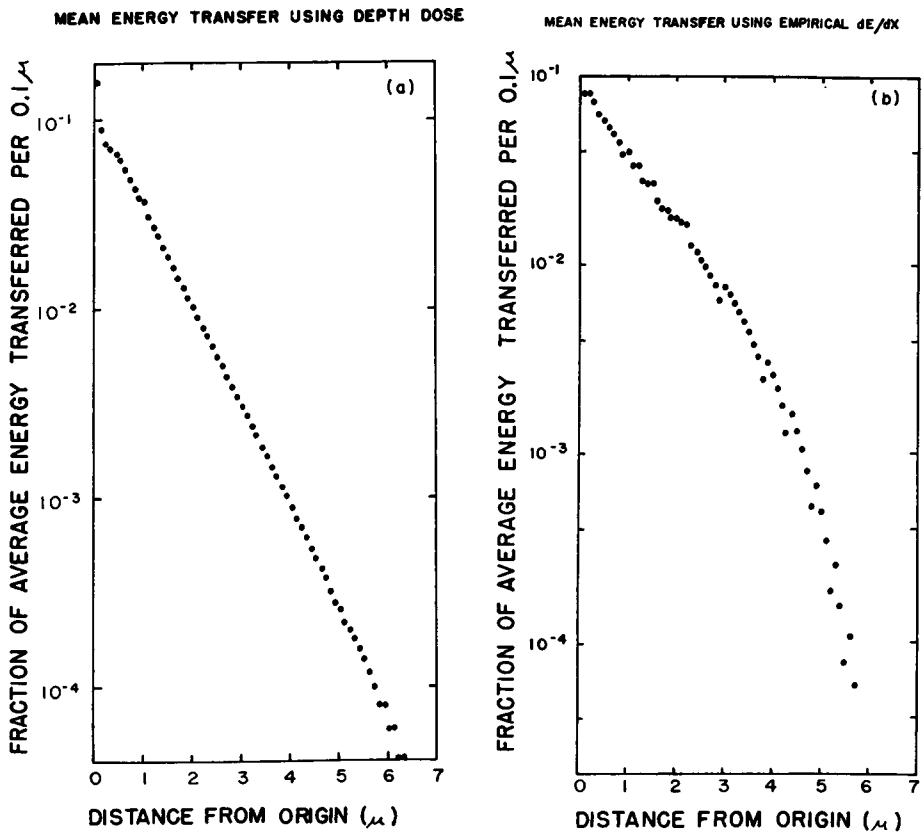

FIGURE 3 The representative energy distribution. The representative energy distribution was determined as described in the text. (*a*) The representative energy distribution used in the calculated tritium energy distributions, incorporating specific energy transfers according to the expressions in Fig. 2. (*b*) A comparative energy distribution, incorporating specific energy transfers according to the distance derivative, dE/dx, given in the legend of Fig. 2.

ing to the relative frequency with which tritium would emit an electron of such an initial energy. This frequency distribution was provided by Fermi's theory of beta decay[1] which has been verified experimentally for tritium by Langer and Moffat (11).

The experimental data on energy transfer from low energy electrons was provided by Dr. A. Cole (personal communication). The data appeared to fall into two classes. For electrons of incident energies 0.15, 0.25, 0.50, 1.05, and 3.0 kev the deposited energy plotted against absorption depth showed one general form (Fig. 2*a*) and for electrons of incident energies 5 kev and greater (up to 18 kev) this plot was more nearly approximated by a second curve (Fig. 2*b*). These two generalized relationships between deposited energy and depth were used to describe the experimental transfer data included in the calculated representative energy distribution for tritium (Fig. 3*a*).

An alternate expression for the energy transfer from electrons of specific initial energies has been suggested (9). However, in this suggestion a similarity between beta particles and more massive charged particles was assumed. It was proposed that the energy transfer be made equivalent to the distance derivative of a range-energy plot. Since the ranges of electrons are somewhat ambiguous because of straggling, and since the actual regions receiving deposited energies are difficult to define, a representative energy distribution for tritium based on this suggestion was not used. Nevertheless, for the sake of comparison a distribution was calculated (Fig. 3*b*). This distribution did not differ greatly from that formulated using depth-dose data.

RESULTS

Results were obtained for the simulated decay of radioisotopes incorporated into as many as seven different labeled regions within the bacterial volume. The positions were selected to represent internal geometries which could possibly be achieved by the incorporation of specific compounds and also some geometries not yet feasible by current experimental techniques. The bacterial volume was defined by L equal to 1.32 μ and R equal to 0.44 μ. This provided a model bacterium having a diameter of 0.88 μ, a length of 2.2 μ, and a total volume of 1.16 μ^3. The model was considered a good approximation of the most frequent bacterial cell found in experimental cultures, as determined by direct optical observations, weight and density determinations, and size-frequency distributions using the Coulter Counter.[2]

Simulated Tritium Decay

The energy distributions recorded for tritium decays varied markedly (Table I). The highest energy densities were recorded in the center of the bacterial volume (sensing volume 1). This occurred when the labeled region was in the center (large nucleus or small nucleus) and amounted to about 1 kev per sensing volume per

---

[1] A nonrelativistic coulomb factor was used (10).

[2] The Coulter Counter is an electronic cell counter manufactured by Coulter Electronics, Inc., Hialeah, Florida.

decay, or about 100 rads per decay (see legend of Table I). Allowing simulated decays to originate in more general regions of the bacterial volume, or in confined regions in more peripheral positions, produced lower maximum energy densities and more uniform distributions throughout the eight sensing volumes. These latter configurations produced a maximum of 35 rads per decay in sensing volume 1.

In general, the energy recorded external to the bacterium was 50–70% of the absorbable energy released by tritium (Table I, last column). Only small variations in the external energy resulted from extreme differences in tritium position within the model. Very little of the external energy is transferred to material at distances greater than about 5 μ from the bacterial surface.

TABLE I

DISTRIBUTIONS OF ENERGIES DEPOSITED BY THE DECAY OF INCORPORATED TRITIUM

	Distribution of energy (*ev*) deposited per decay								
	Sensing volumes								External to bacterial volume
Labeled region	1	2	3	4	5	6	7	8	
Small nucleus	1018	635	397	217	156	128	132	92	2925
Large nucleus	924	659	410	239	142	131	140	100	2955
Average nucleus	971	647	404	228	149	130	136	96	2939
Whole cell	354	307	315	299	198	249	198	194	3586
Cytoplasm	183	245	282	279	338	266	270	197	3640
Middle cell	229	394	421	464	298	243	277	123	3251
Thin cell wall	104	107	139	147	240	262	249	340	4112
Thick cell wall	95	112	160	168	234	262	303	293	4073
Average cell wall	100	110	150	158	237	262	276	317	4090

The energies listed are normalized so that the total energy in any one distribution equals 5.7 kev, the average energy of one tritium beta particle (12). The tabulated energies may be converted to rads per decay by multiplying by 0.102. This factor converts the values in the table to rads, using a bacterial density of 1.08 g/cc and the fact that each sensing volume is 0.145 μ^3. The various positions are defined by the following values of r_1 and r_2 (respectively): 0.000 and 0.222 for small nucleus, 0.000 and 0.238 for large nucleus, 0.000 and 0.440 for whole cell, 0.220 and 0.440 for cytoplasm, 0.238 and 0.325 for middle cell, 0.415 and 0.440 for thin cell wall, and 0.400 and 0.440 for thick cell wall. Average nucleus and average cell wall are the averages of the two values for the nucleus and the two values for the cell wall, respectively.

Energy deposits within the bacterial volume were also calculated for simulated tritium decays originating only in the external medium. No significant variations in the energy density as recorded in the eight sensing volumes were noted (data not given here). The average energy density in the bacterial volume was 0.65–0.70 times that in the medium. This corresponded to approximately 1 rad in the bacterium per 1.5×10^{10} decays per ml of medium.

Simulated Decay of Other Isotopes

Energy distributions in the biological volume resulting from simulated ^{14}C, ^{35}S, and

^{32}P decay also were determined. For these more energetic beta emitters, however different representative energy distributions were used.

Representative energy distributions for ^{14}C and ^{35}S were calculated as described under Fig. 3*b*. The results showed exponential absorptions very similar to those found experimentally by Libby (13). Both representative energy distributions showed less than 5 % variation over a distance of 1 μ. A representative energy distribution for ^{32}P was not calculated because experimental data indicated there would be less than 1 % variation in energy transfer over the first micron (14). Consequently, representative energy distributions having constant energy transfers were used to represent ^{14}C, ^{35}S, and ^{32}P. This was considered a good approximation to the real distributions over the distances required by the model bacterium.

TABLE II

DISTRIBUTIONS OF ENERGY DEPOSITED BY THE DECAY OF INCORPORATED ^{14}C, ^{35}S, AND ^{32}P

		Distribution of energy (*ev*) deposited per decay							
		Sensing volumes							
Labeled region	Isotope	1	2	3	4	5	6	7	8
Small nucleus	^{14}C	183	123	90	53	39	35	38	26
	^{35}S	174	117	86	50	37	33	36	25
	^{32}P	33	22	16	10	7	6	7	5
Cytoplasm	^{14}C	48	55	60	55	66	53	54	42
	^{35}S	45	52	57	53	63	50	52	40
	^{32}P	9	10	11	10	12	10	10	8
Thick cell wall	^{14}C	29	33	50	41	39	51	61	56
	^{35}S	28	32	47	40	37	48	58	54
	^{32}P	5	6	9	8	7	9	11	10
Whole cell	^{14}C	73	65	79	61	68	52	45	42
	^{35}S	70	62	76	58	64	50	43	40
	^{32}P	13	12	14	11	12	10	8	8

This table is similar to Table I, except that the energy distributions are those for the radioisotopes ^{14}carbon, ^{35}sulfur, and ^{32}phosphorus. As described in the text, a constant rate of energy transfer was used in the calculations for these isotopes. These rates were 99 ev/0.1 μ for ^{14}C, 94 ev/0.1 μ for ^{35}S, and 18 ev/0.1 μ for ^{32}P.

The energy distributions calculated for these isotopes, occupying various configurations within the bacterial volume (Table II), generally showed less energy recorded per decay in every sensing volume, compared to the results for tritium. Moreover, the distributions showed somewhat smaller variations in energy density.

DISCUSSION

The procedure (computer program) used to determine the results reported here was verified by seeking certain results that could also be obtained by analytical means.

This was greatly facilitated in many instances by allowing the cylindrical region of the bacterial volume to have zero length, thereby producing a spherical volume. In all trials the procedure executed by the computer gave results within a few percent of those deduced analytically.

The dimensions of the bacterial volume and the density of the absorbing material used in the calculations were established according to measurements of a multi-auxotroph of *E. coli* strain 15 called WWU. It is also known of WWU that colony-forming ability is inactivated by 50 kev X-rays with a mean lethal dose of 4.5 krads (unpublished results), in conditions of temperature and environment similar to those in which the same strain is inactivated by the decay of incorporated thymidine-^{3}H, uracil-^{3}H, and ^{3}H-amino acids with killing efficiencies of 1.35, 1.05, and 0.73%, respectively (15). The killing efficiencies for the different tritium compounds correspond to mean lethal numbers of decays per bacterium of: 75 for thymidine-^{3}H, 95 for uracil-^{3}H, and 137 for ^{3}H-amino acids.

The results in Table I indicate that these numbers of decays would be accompanied by radiation doses in the bacterial cell ranging from 1 to 10 krads. However, if the following assumptions are made as to the positions occupied in the bacterial volume by the different incorporated tritium compounds and the location of the material receiving lethal radiation produced events, a single mean lethal dose is suggested: (*a*) Assume thymidine-^{3}H is 0.8 in the "average nucleus" and 0.2 in the "whole cell." (*b*) Assume uracil-^{3}H is 0.8 in the "whole cell" and 0.2 in the "average nucleus." (*c*) Assume ^{3}H-amino acids are 0.8 in the "whole cell" and 0.2 in the "average cell wall." (*d*) Assume loss of colony-forming ability is produced by an ionization event in sensing volume 1 or 2. Accordingly, the reported killing efficiencies correspond to mean lethal radiation doses of 5460 rads for thymidine-^{3}H, 4133 rads for uracil-^{3}H, and 3987 rads for ^{3}H-amino acids, or an average equal to approximately 4.5 krads.

Inasmuch as the assumptions employed do not seem too unreasonable (6, 16–18), and the calculated mean lethal doses for the three known killing efficiencies are similar to one another and to the experimental mean lethal dose under X-rays, the killing produced by these tritium compounds is apparently mediated solely by radiation doses to the bacterial nucleus. Hence, the earlier suggestion by Koch (5) that differential killing efficiencies are the result of differential dose rates to the cell nucleus is substantiated by these calculations.

In way of contrast, these calculations do not lead to a simple explanation for the differential mutation production found in WWU. The efficiency of mutagenesis (per decay) for incorporated uracil-^{3}H is 2.8 times that for incorporated thymidine-^{3}H and 6.6 times that for incorporated ^{3}H-amino acids (15). From the assumptions given above with regard to the position of different incorporated tritium compounds, per decay doses may be calculated in all eight sensing volumes (Fig. 4). In none of these volumes is the dose predicted for one compound six times that predicted for

another compound. The calculations therefore support the proposal that the high level of mutation production by uracil-^{3}H is greatly facilitated by a local effect resulting from the decay of tritium at the 5-position of the pyrimidine ring (8).

The calculations in Table II for the more energetic beta emitters ^{14}C, ^{35}S, and ^{32}P also show differential dose rates, but the amount of energy deposited in the bacterium per decay is considerably less than from tritium.

Fig. 4 shows in graphical form the calculated energy distributions which might be expected in bacteria labeled with thymidine-^{3}H, uracil-^{3}H, or ^{3}H-amino acids. These results show large variations in energy deposition as a function of the location of the labeled compound in the cell and the location of the sensitive target. The degree to which these variations in energy deposition may be utilized are of course limited by the precision with which tritium may be incorporated into specific regions of the bacterium. However, as indicated above these variations seem to be sufficient to explain differential killing efficiencies. In addition, they support the conclusion re-

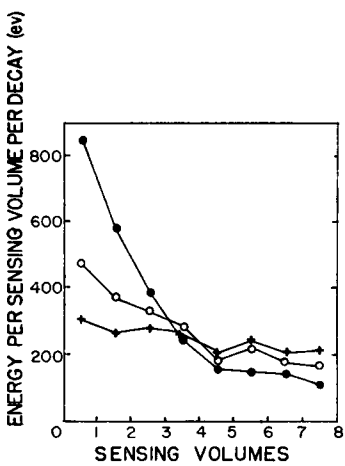

FIGURE 4 Approximate energy distributions predicted for the decay of incorporated tritium compounds. The results of Table I were used to approximate energy distributions from tritium incorporated as thymidine-^{3}H (●), uracil-^{3}H (○), or ^{3}H-amino acids (+). The assumptions regarding the labeled regions produced by these compounds are given in the text. The eight sensing volumes are graphically represented in Fig. 1*b*.

garding DNA degradation drawn by Person and Sclair (19). DNA degradation resulting from the decay of incorporated tritium compounds should vary with the compound incorporated, as described, if the radiation-induced event responsible for degradation occurs in the nuclear region. Lastly, these variations in energy deposition have been cited to explain the differential proportions of two arginine revertant types resulting from the decay of different tritium compounds (20). As may be seen in Fig. 4, two radiosensitive targets occupying different positions in the cell would be exposed to specific differential doses, depending on the mode of tritium incorporation.

The authors would like to thank S. Phillips, B. Benson, and W. Yeisley for their helpful interest in the logic of the computer program and Drs. A. Cole, F. Hutchinson, and E. Pollard for their com-

ments and ideas regarding energy transfer by low energy electrons. The authors are most grateful for the data supplied by Dr. Cole. The very excellent services provided by the Computer Science Department of The Pennsylvania State University are acknowledged. This work was supported by NASA grant NSG-324.

Received for publication 27 April 1968 and in revised form 7 June 1968.

REFERENCES

1. STENT, G. S., and C. R. FUERST. 1960. *Advan. Biol. Med. Phys.* **7**:1.
2. STRAUSS, B. S. 1958. *Radiation Res.* **8**:234.
3. APELGOT, S., and M. DUQUESNE. 1963. *Intern. J. Radiation Biol.* **7**:1.
4. STEWART, F. S. 1964. *Intern. J. Radiation Biol.* **8**:545.
5. KOCH, A. L. 1965. *Radiation Res.* **24**:398.
6. PERSON, S. 1963. *Biophys J.* **3**:183.
7. RACHMELER, M., and A. B. PARDEE. 1963. *Biochim. Biophys. Acta.* **68**:62.
8. PERSON, S., and R. C. BOCKRATH, JR. 1965. *J. Mol. Biol.* **13**:600.
9. ROBERTSON, J. S., and W. L. HUGHES. 1959. Proceedings of the First National Biophysics Conference. Yale University Press, New Haven, Conn.
10. EVANS, R. D. 1955. The Atomic Nucleus. McGraw-Hill Book Co., Inc. New York.
11. LANGER, L. M., and R. J. D. MOFFAT. 1952. *Phys. Rev.* **88**:689.
12. JENKS, G. H., J. A. GHORMLEY, and F. H. SWEETON. 1949. *Phys. Rev.* **75**:701.
13. LIBBY, W. F. 1956. *Phys. Rev.* **103**:1900.
14. SOMMERMEYER, K., and K. H. WAECHTER. 1953. *Z. Angew. Phys.* **5**:242.
15. PERSON, S., and R. C. BOCKRATH, JR. 1964. *Biophys. J.* **4**:355.
16. FRANKLIN, R. M., and N. GRANBOULAN. 1965. *J. Mol. Biol.* **14**:623.
17. CARO, L. G. 1961. *J. Biophys. Biochem. Cytol.* **9**:539.
18. MAAØE, O., and N. O. KJELDGAARD. 1966. Control of Macromolecular Synthesis. W. A. Benjamin, Inc., New York. 189.
19. PERSON, S., and M. H. SCLAIR. 1968. *Radiation Res.* **33**:66.
20. BOCKRATH, R. C. 1967. *Mutation Res.* **4**:871.